United Mechanisms for the Generation of Low- and High-Frequency Tropical Waves. Part I: Control Experiments with Moist Convective Adjustment

Y. HAYASHI AND D. G. GOLDER

Geophysical Fluid Dynamics Laboratory/NOAA, Princeton University, Princeton, New Jersey

(Manuscript received 11 December 1995, in final form 23 October 1996)

ABSTRACT

To examine several mechanisms for the generation of low- and high-frequency tropical waves, numerical experiments are conducted using an idealized nine-level R21 spectral model with the original scheme of moist convective adjustment (MCA). The model prescribes globally uniform, time-independent distributions of sea surface temperatures and insolation, thereby excluding stationary waves and extratropical baroclinic waves. The idealized model, however, still produces tropical intraseasonal oscillations, superclusters, Kelvin waves, and mixed Rossby–gravity waves.

When eliminating the wind fluctuations in the parameterized surface fluxes of latent and sensible heat, the intraseasonal oscillations are profoundly weakened while other waves are not substantially weakened. Subsequently, the MCA scheme is modified to neutralize any conditionally unstable stratification that would otherwise develop during periods of nonsaturation. This modification suppresses the part of the MCA process that neutralizes, upon saturation, any preexisting unstable stratification. In spite of the presence of moisture convergence, all tropical transient waves then disappear, in contrast to the wave-CISK (conditional instability of the second kind) mechanism.

The above results are consistent with the united mechanisms proposed as follows. Intraseasonal oscillations are maintained primarily through the evaporation–wind feedback mechanism. Other waves are maintained primarily through the ''saturation-triggering mechanism'' and/or the lateral-triggering mechanism. The saturation-triggering mechanism hypothesizes that transient waves can be triggered by the intermittent onset of nonequilibrium moist convection, upon saturation, to neutralize any preexisting unstable stratification.

1. Introduction

Tropical transient disturbances consist of periodic, quasiperiodic, and nonperiodic oscillations. Periodic oscillations consist of diurnal and annual cycles along with their higher harmonics. Examples of tropospheric quasiperiodic oscillations are the 4–5-day easterly wave (Riehl 1954), the 40–50 day tropical intraseasonal oscillation (TIO) (Madden and Julian 1971, 1972), and the 25–30 day TIO (Hayashi and Golder 1986, 1988, 1993). Among the nonperiodic waves are superclusters (Nakazawa 1988; Hayashi and Nakazawa 1989), cloud clusters, and gravity waves, having a wide wavenumber–frequency range. Examples of stratospheric quasiperiodic oscillations are the 4–5-day mixed Rossby–gravity (MRG) wave (Yanai and Maruyama 1966) and the 10–20-day Kelvin wave (Wallace and Kousky 1968). In the present paper, the term ''MRG waves'' refers to vertically propagating MRG waves that extend from the troposphere to the stratosphere, not the tropospherically confined MRG waves (e.g., Hendon and Liebman 1991; Randel 1992). Reviews of observed tropical transient waves have been presented by Wallace (1971, 1973), Yanai (1975), and Madden and Julian (1994).

Since the initiation of basic equatorial-wave theory (e.g., Matsuno 1966; Lindzen 1967; Lindzen and Matsuno 1968), a number of theories have been proposed to explain tropical stratospheric and tropospheric transient waves. Most of the existing theories, except those for easterly waves, can be classified as follows:

1) Lateral-forcing theory, which studies the response of tropical waves to prescribed lateral forcing.
   (a) Periodic lateral forcing (e.g., Charney 1969; Bennet and Young 1971; Wilson and Mak 1984; Zhang and Webster 1989, 1992; Zhang 1993).
   (b) Random lateral forcing (e.g., Mak 1969; Hayashi 1976; Itoh 1978).
2) Thermal-forcing theory, which studies the response of tropical waves to prescribed thermal forcing.
   (a) Periodic thermal forcing (e.g., Holton 1972; Yamagata and Hayashi 1984; Hayashi and Miyahara 1987; Webster and Chang 1988; Itoh and Nishi 1990; Itoh 1994; Hendon and Salby 1996).

Corresponding author address: Dr. Yoshikazu Hayashi, Geophysical Fluid Dynamics Laboratory/NOAA, Princeton University, P.O. Box 308, Princeton, NJ 08542.
E-mail: yh@gfdl.gov

(b) Random thermal forcing (e.g., Holton 1973; Hayashi 1976; Chang 1976; Itoh 1977).
(c) Episodic thermal forcing (Salby and Garcia 1987; Garcia and Salby 1987; Horinouchi and Yoden 1996).
(d) Impulsive thermal forcing (Bretherton and Smolarkiewicz 1989; Nicholls et al. 1991; Pandya et al. 1993; Bretherton 1993; Mapes 1993).

3) Wave-instability theory, which studies the instability of tropical waves coupled with moist convection, condensation, and evaporation.
(a) High-frequency wave-CISK (conditional instability of the second kind) (e.g., Yamasaki 1969; Hayashi 1970; Lindzen 1974; Kuo 1975; Steven and Lindzen 1978; Davis 1979).
(b) Low-frequency wave-CISK (e.g., Lau and Peng 1987; Miyahara 1987; Takahashi 1987; Yamagata 1987; Chang and Lim 1988; Wang 1988; Hendon 1988; Itoh 1989; Lau et al. 1989; Davey 1989; Lim et al. 1990; Yoshizaki 1991; Dunkerton and Crum 1991; Crum and Dunkerton 1992, 1994; Frederiksen and Frederiksen 1993; Blade and Hartmann 1993; Cho 1994; Wang and Li 1994; Salby et al. 1994; Xie 1994; Lau and Wu 1994).
(c) Evaporation–wind feedback instability (e.g., Neelin et al. 1987; Emanuel 1987, 1993; Yano and Emanuel 1991; Goswami and Goswami 1991, 1996; Xie et al. 1993a,b; Neelin and Yu 1994; Yu and Neelin 1994).

A brief review of the above theories can be found in Hayashi and Golder (1993). In particular, wave-CISK theory has been critically evaluated by Emanuel et al. (1994) and Chao (1995). This instability is crucially dependent on the wave-CISK parameterization of moist convection in terms of large-scale moisture convergence. Wave-CISK theory is consistent with the Kuo (1965) scheme, since the wave-CISK parameterization is essentially a simplification of the Kuo scheme. In the presence of strong cumulus friction, however, only synoptic-scale wave-CISK modes grow (Steven and Lindzen 1978). This instability does not occur at all in the linear model of Neelin and Yu (1994), which employs the Betts–Miller scheme (Betts 1986; Betts and Miller 1986). It is also virtually absent from other linear models (Stark 1976; Bates et al. 1978; Crum and Stevens 1983) that use the Arakawa–Schubert (1974) scheme. Moreover, if a time lag is allowed in the response of convective heating to the large-scale field, net cooling and wave damping occur in the absence of the evaporation–wind feedback (EWF) mechanism (Emanuel 1993; Yu and Neelin 1994). Neelin et al. (1987) demonstrated, using a low-resolution idealized general circulation model with moist convective adjustment (MCA), that the tropical 25–30-day TIO appearing in the model is substantially weakened when the EWF mechanism is eliminated. It was not determined, however, whether the weak amplitudes that occurred in the presence of MCA were due to the wave-CISK mechanism or some other mechanisms.

Numerical simulations of tropical transient waves relevant to the present study include the following papers. For Kelvin and MRG waves, see Hayashi (1974), Tsay (1974), Hayashi and Golder (1978, 1980, 1994), Hayashi et al. (1984), Itoh and Ghil (1988), Boville and Randel (1982), Hess et al. (1993a,b), and Manzini and Hamilton (1993). For intraseasonal oscillations, see Hayashi and Golder (1986, 1988, 1993), Lau and Lau (1986), Hayashi and Sumi (1986), Neelin et al. (1987), Pitcher and Geisler (1987), Lau et al. (1988), Swinbank et al. (1988), Kuma (1990, 1994), Tokioka et al. (1988), Park et al. (1990), Slingo and Madden (1991), Sumi (1992), Yip and North (1993), Chao and Lin (1994), Seager and Zebiak (1994), Brown and Bretherton (1995), Sheng (1996), and Slingo et al. (1996). For superclusters, see Hayashi and Sumi (1986), Numaguti and Hayashi (1991a,b), Sumi (1992), Kuma (1994), Hayashi and Golder (1993, 1994), Chao and Lin (1994), Yano et al. (1995), and Chao and Deng (1996). For cloud clusters, see Yamasaki (1977), Nakajima and Matsuno (1988), and Xu (1993). For gravity waves, see Hayashi et al. (1984), Hayashi et al. (1989), Miyahara et al. (1986), Hamilton and Mahlman (1988), Held et al. (1993), Takahashi (1993), and Takahashi and Shiobara (1995).

These simulations are based on either realistic or idealized models that use different schemes of moist convection and different resolutions. From the analyses of realistic Geophysical Fluid Dynamics Laboratory (GFDL) general circulation models with MCA, which simulated Kelvin and MRG waves, TIOs, and superclusters, the following results have been obtained (Hayashi 1974; Hayashi and Golder 1986, 1988, 1993, 1994; Manzini and Hamiliton 1993).

1) The simulated precipitation and evaporation do not exhibit distinct periodicities corresponding to Kelvin and MRG waves, being consistent with nonperiodic thermal-forcing theories but contrary to instability theories.
2) The Fourier components of simulated tropospheric convective heating and vertical velocities corresponding to TIOs, Kelvin waves, and MRG waves are nearly in phase, being consistent with instability theories but contrary to nonperiodic thermal-forcing theories.
3) The simulated precipitation and evaporation exhibit distinct periodicities corresponding to TIOs, being consistent with instability theories but contrary to nonperiodic thermal-forcing theories.

Since none of the existing theories can adequately explain tropical low- and high-frequency waves, Hayashi and Golder (1994) proposed the ''united mechanisms,'' which consist of the EWF mechanism, the ''sat-

uration-triggering (ST) mechanism,'' and the lateral-triggering mechanism. The EWF mechanism assumes that tropical transient waves, coupled with quasi-equilibrium moist convection, can grow through the wave instability resulting from the interaction between surface evaporation and the low-level wind. The ST mechanism assumes that tropical transient waves can be triggered and resonantly amplified by the intermittent onset of nonequilibrium moist convection upon saturation. The onset neutralizes any preexisting conditionally unstable stratification that has developed during periods of nonsaturation. The intermittency results from the assumption that moist convection does not occur during periods of nonsaturation. The lateral-triggering mechanism assumes that tropical transient waves can be triggered and resonantly amplified by lateral forcing extending from the extratropics.

To examine the united mechanisms, the present study has conducted numerical experiments with the use of an idealized R21 spectral model having the original MCA scheme. The idealized model has globally uniform, time-independent sea surface temperatures and equinox insolation conditions, thereby excluding stationary waves, diurnal and annual oscillations, and extratropical baroclinic waves. The model, however, still produces intraseasonal oscillations, superclusters, Kelvin waves, and MRG waves. The lateral-triggering mechanism is not examined here, since the model does not produce extratropical disturbances. In the future, a realistic model will be used to reexamine the united mechanisms, including the lateral-triggering mechanism.

Since the present results are based on an idealized model atmosphere and are sensitive to the choice of the moist convective scheme, they are not directly applicable to the real atmosphere. Nevertheless, this study is a step toward uniting plausible wave-generation mechanisms that occur in the real atmosphere.

Section 2 describes the experimental procedure, while section 3 presents the experimental results. Section 4 is devoted to discussion, and section 5 presents conclusions and remarks.

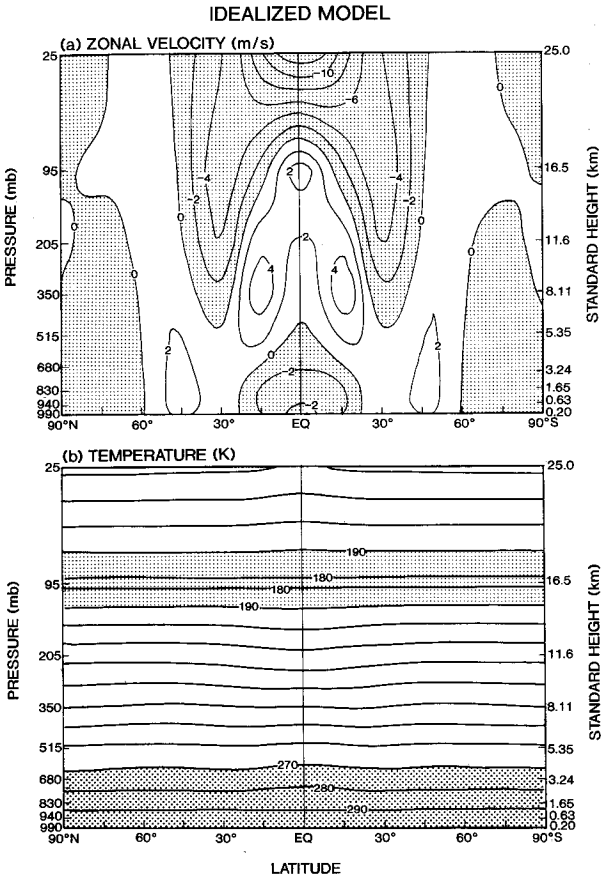

FIG. 1. Latitude–height distributions (5-yr average) of (a) the zonal-mean zonal wind and (b) zonal-mean temperature of the idealized model. The contour value for (a) is 2 m s^{-1}, with light shading indicating negative interval (easterlies). The contour interval for (b) is 10 K, with dark shading indicating values greater than 270 K and light shading values less than 190 K.

2. Experimental procedure

a. Idealized model

The idealized model, which was used for the control experiment (experiment 1), was constructed by simplifying a nine-level GFDL spectral general circulation model with rhomboidal truncation at zonal wavenumber 21 (R21) that employs the original MCA scheme (Manabe et al. 1965). Detailed descriptions of the realistic model can be found in Manabe et al. (1979) and Gordon and Stern (1982). The idealized model has globally uniform sea surface temperatures of 300 K, insolation, and gaseous absorbers, thereby eliminating stationary waves and extratropical baroclinic waves. The insolation conditions and distributions of the absorbing gases were fixed at equatorial equinox values. No cloud–radiation feedback was incorporated.

Figure 1 shows the latitude–height distributions of the (a) zonal-mean zonal velocity and (b) temperature averaged over a 5-yr integration of the idealized model. In Fig. 1a, weak easterlies (-2 m s^{-1}) appear in the lower tropical troposphere, while the vertical shear is extremely weak in the extratropics. Although the zonal-mean easterlies are weaker than those observed (-5 m s^{-1}), they are comparable to the local low-level easterlies found over the convectively active western Pacific. The low-level flow is easterly and therefore satisfies the condition for eastward-moving TIOs to grow through the EWF instability mechanism (Neelin et al. 1987; Emanuel 1987).

In Fig. 1b, small latitudinal variations appear in the mean-temperature field, in spite of the uniform sea surface temperature and insolation conditions. These temperature variations result from the adiabatic heating due to mean meridional circulations, which probably result from wave–mean flow interactions. Interestingly, the

mean upward motion (not illustrated) is concentrated between 7°N and 7°S, resembling the Hadley cell. The tropopause occurs at approximately 100 mb at all latitudes. The temperature of the equatorial tropopause is 178 K, which is about 12 K colder than that (190 K) of the realistic model under equinox conditions and about 22 K colder than that (200 K) observed. The effect of this unrealistic feature on intraseasonal oscillations will be discussed in section 3h.

b. Experiments

Five fundamental experiments (experiments 1–5), including the control experiment (experiment 1), were conducted with the use of the idealized model. In addition, several supplementary experiments were performed to clarify the results of the fundamental experiments.

In experiment 2, the idealized model was modified in such a way as to eliminate the EWF mechanism by suppressing the wind fluctuations in the surface fluxes of latent and sensible heat (i.e., ''wind-feedback removal''), following Neelin et al. (1987). This was accomplished by replacing the low-level winds in the parameterized surface fluxes of latent and sensible heat with the zonal- and time-mean equatorial value of the lowest-level wind taken from experiment 1.

In experiment 3, the idealized model was modified as in experiment 2 to eliminate the EWF mechanism. In addition, the wave-CISK mechanism was eliminated by replacing vertical moisture advection with its zonal mean at each time step and then predicing the moisture. As is explained in the appendix, this modification only removes the feedback of the horizontal convergence of winds to the fluctuations of moisture convergence. This feedback (i.e., ''convergence feedback''), which is part of the moisture convergence, is crucial to wave-CISK. The horizontal moisture advection, which is not crucial to wave-CISK, is not modified. This experiment, therefore, should not be interpreted as completely eliminating the moisture-convergence or moisture-advection fluctuations.

In experiment 4, the idealized model was modified as in experiment 2 to remove the EWF mechanism. In order to remove the ST mechanism, the scheme of MCA was also modified to always neutralize any conditionally unstable stratification that would otherwise develop during periods of nonsaturation. The MCA process can be interpreted as consisting of two consecutive processes. The first MCA process neutralizes, upon saturation, any preexisting conditionally unstable stratification that has developed during periods of nonsaturation. Subsequently, the second MCA process continually neutralizes any conditionally unstable stratification predicted during periods of saturation. The modified MCA scheme suppresses the first process, while allowing the second process. In practice, this is accomplished by allowing MCA and large-scale condensation to occur, even during periods when nonsaturation is predicted in the absence of condensation. This procedure eliminates not only the ST mechanism, but also artificially allows both positive and negative values of condensation in such a way that the atmosphere becomes always saturated.

In experiment 5, the idealized model was modified as in experiment 2 to remove the EWF mechanism. In contrast to experiment 4, however, experiment 5 eliminates only the ST mechanism while retaining the positive-only property of condensational heating. In practice, the process of dry convective adjustment, which is part of the MCA scheme, was modified by replacing the dry adiabat with the moist adiabat. The modified dry-adjustment process continually neutralizes any conditionally unstable stratification that would otherwise develop during periods of nonsaturation, thereby suppressing the first MCA process while allowing the second MCA process.

In experiments 1 and 2, the models were integrated over a period of 5 years to obtain statistically stable wavenumber-frequency spectra, while experiments 3–5 were integrated over a 1-yr period to obtain time-dependent wavenumber kinetic energy. The initial conditions for experiment 1 were taken from the end of a 1-yr spinup integration of the idealized model. The initial conditions for experiments 2–5 were taken from the last day of the fourth year of integration of the idealized model (experiment 1).

Using once-daily output data, space–time spectra were computed by the maximum entropy method (see Hayashi 1982). To enhance Kelvin modes, the equatorially symmetric component (i.e., the half-sum of Northern and Southern Hemispheric values) was extracted from the zonal velocity, vertical velocity, and convective heating, following the procedure proposed by Yanai and Murakami (1970). To enhance MRG modes, the equatorially symmetric component was extracted from the meridional velocity, while the equatorially antisymmetric component (i.e., the half-difference between Northern and Southern Hemispheric values) was extracted from the vertical velocity and convective heating.

3. Results

To examine the effects of several mechanisms on the transient kinetic energy, Fig. 2 shows transient kinetic energy as a function of time for three ranges of zonal wavenumbers: 1–4 (top), 5–9 (middle), and 10–21 (bottom). The energey has been integrated in the vertical and over latitudes 10°N–10°S, and smoothed by an 11-day running mean. In this figure, experiment 1 refers to year 5 of the idealized model. The initial conditions for experiments 2–5 were taken from the last day (labeled day 0) of the fourth year of the idealized model. Wavenumbers 1–4 include intraseasonal oscillations and shorter-period components such as 10–20-day Kelvin waves. Wavenumbers 5–9 comprise superclusters and mixed Rossby–gravity waves, while wavenumbers 10–21 represent high-wavenumber components.

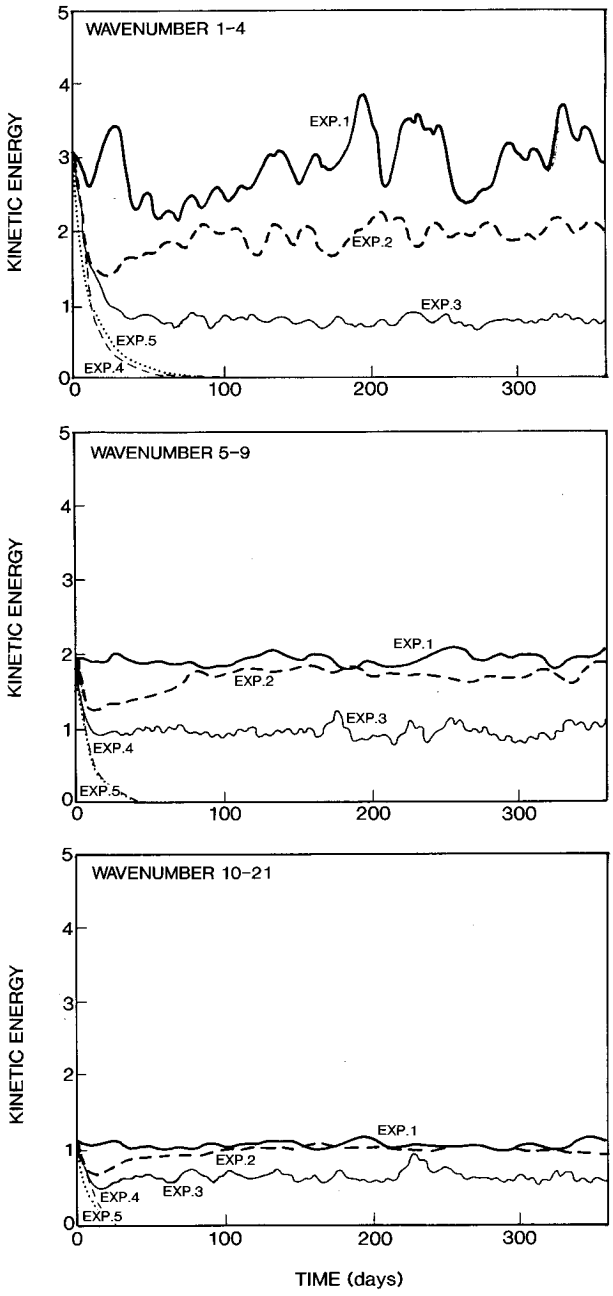

FIG. 2. Time distribution (day 0–360) of transient kinetic energy (units 10^4 J m^{-2}) for wavenumbers 1–4 (top), 5–9 (middle), and 10–21 (bottom). The energy has been integrated in the vertical and over latitudes 10°N–10°S, and smoothed by an 11-day running average. The thick solid lines indicate experiment 1 (idealized model), thick dashed lines experiment 2, thin solid lines experiment 3, thin dashed lines experiment 4, and thin dotted lines experiment 5. The initial conditions for experiments 2–5 were taken from the last day (labeled day 0) of the fourth year of integration of the idealized model.

a. Effect of wind feedback

As can be seen in Fig. 2, the transient kinetic energy for wavenumbers 1–4 of experiment 1 (thick solid line) is substantially reduced by the removal of wind feedback in experiment 2 (thick dashed line). As will be shown later, this substantial reduction is essentially due to the pronounced reduction of the wavenumber 1 40–50-day TIO component, which accounts for only part of the wavenumber 1–4 component. For wavenumbers 5–9 and 10–21, in contrast, the transient kinetic energy is not substantially reduced by the wind-feedback removal.

b. Effect of convergence feedback

In experiment 3, convergence feedback, which is crucial to the wave-CISK mechanism, was removed in addition to the wind-feedback removal, although moisture convergence was not entirely removed. Convergence feedback not only reduces the effective value of static stability, but also affects the onset of saturation and moist convection. As can also be seen in Fig. 2, the transient kinetic energy is substantially reduced by the additional removal of convergence feedback for all wavenumber ranges in experiment 3 (thin solid line). Even in the absence of the wave-CISK mechanism, however, the transient kinetic energy is not completely dissipated, although the fluctuations in precipitation are drastically reduced (not illustrated). This result demonstrates that another mechanism must exist in the idealized model to generate transient kinetic energy in the absence of the wave-CISK, EWF, and lateral-triggering mechanisms.

c. Effect of the saturation triggering mechanism

To examine the ST mechanism, experiments 4 and 5 eliminated in different manners as described in section 2, in addition to the wind-feedback removal, any conditionally unstable stratification that would otherwise develop during periods of nonsaturation. Convergence feedback, however, was not removed.

As can be seen in Fig. 2, the transient kinetic energy is completely dissipated for all wavenumber ranges in both experiment 4 (thin dashed lines) and experiment 5 (dotted lines), in spite of the presence of convergence feedback. This result demonstrates that the transient kinetic energy in experiment 2 is generated through the ST mechanism in the absence of the EWF and lateral-triggering mechanisms. It also demonstrates that the MCA scheme does not allow wave-CISK that would generate wave energy in the absence of the EWF, ST, and lateral-triggering mechanisms.

d. Tropical intraseasonal oscillations

Figure 3a is based on the results of experiment 1, showing the frequency–height distribution of the wavenumber 1 space–time power spectral density over 5 years of the equatorially symmetric 205-mb zonal velocity averaged between 10°N and 10°S. This figure exhibits a pronounced 40–50-day peak for the eastward-

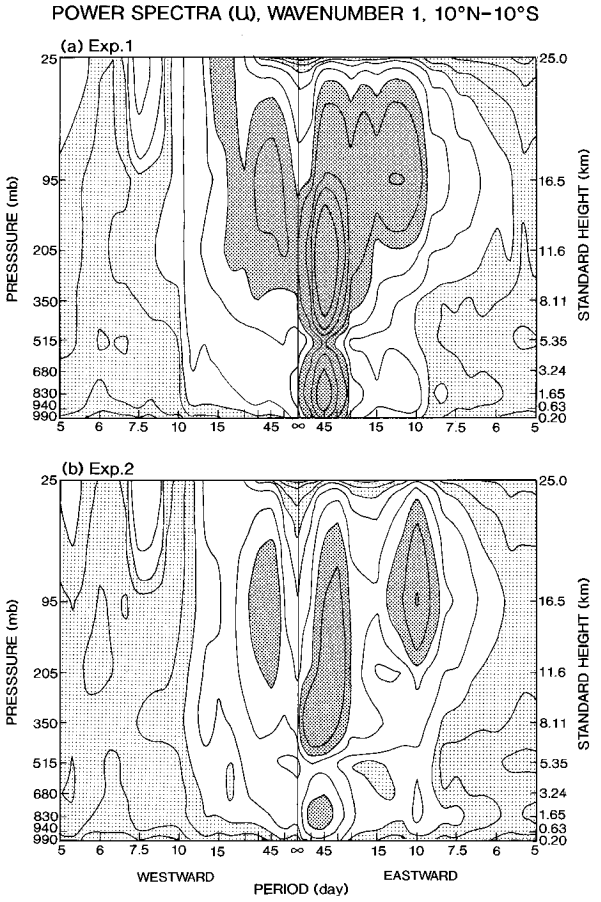

FIG. 3. Frequency–height distributions of the space–time wavenumber 1 power spectral density of the equatorially symmetric zonal velocity averaged between 10°N and 10°S for (a) experiment 1 and (b) experiment 2. Contour values are 0.1, 0.2, 0.5, 1, 2, 5, 10, 20, 50, 100, 200, and 500 $(\text{m s}^{-1})^2$ day. Dark shading indicates values greater than 10, light shading less than 1.

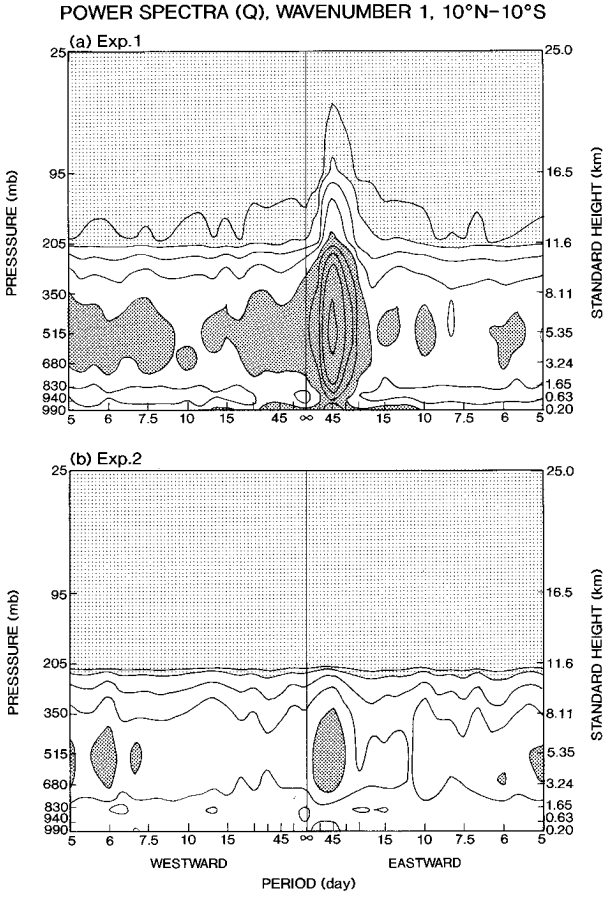

FIG. 4. As in Fig.3 except for the equatorially symmetric MCA heating (Q). Contour values: 0.01, 0.02, 0.05, 0.1, 0.2, 0.5, 1, 2, and 5 $(\text{K day}^{-1})^2$ day. Dark shading indicates values greater than 0.2, light shading less than 0.02.

moving component in both the lower and upper troposphere, corresponding to the observed 40–50-day TIO. Since the wavenumber 1 component of the observed (Nakazawa 1986) and simulated (Hayashi and Golder 1986) TIO has a dominant 40–50-day period, the wavenumber 1 component of the idealized TIO should also have a 40–50-day period, provided that the TIO is a linear wave. The phase velocity of the localized TIO observed in convective regions, however, is slower than the idealized phase velocity, since the localized TIO consists of multiple wavenumber components having the same period.

Fiqure 3b is the same as Fig. 3a, except for experiment 2, which removes wind feedback. Comparison between Figs. 3a (experiment 1) and 3b (experiment 2) indicates that the 40–50-day TIO is profoundly weakened by the wind-feedback removal. This result demonstrates that the simulated 40–50-day TIO is maintained primarily through the EWF mechanism.

e. Kelvin waves

Figure 3a also reveals a stratospheric peak at eastward-moving periods of 10–15 days, corresponding to the 10–20-day Kelvin wave (Wallace and Kousky 1968). Comparison between Figs. 3a (experiment 1) and 3b (experiment 2) indicates that the Kelvin wave peak is not appreciably reduced by the wind-feedback removal, in contrast to the 40–50-day TIO. Since waves in experiment 2 are maintained entirely through the ST mechanism, this result demonstrates that the Kelvin wave in experiment 1 is maintained almost entirely through the ST mechanism. It is also seen that the tropospheric TIO in experiment 2 has as much variance as the stratospheric Kelvin wave. This result suggests that the ST mechanism contributes as much variance to the tropospheric TIO as it does to the stratospheric Kelvin wave, although the TIO is maintained primarily through the EWF mechanism.

Figures 4a and 4b are the same as Figs. 3a and 3b, respectively, except for the symmetric MCA heating (Q). Figure 4a displays a pronounced spectral peak at

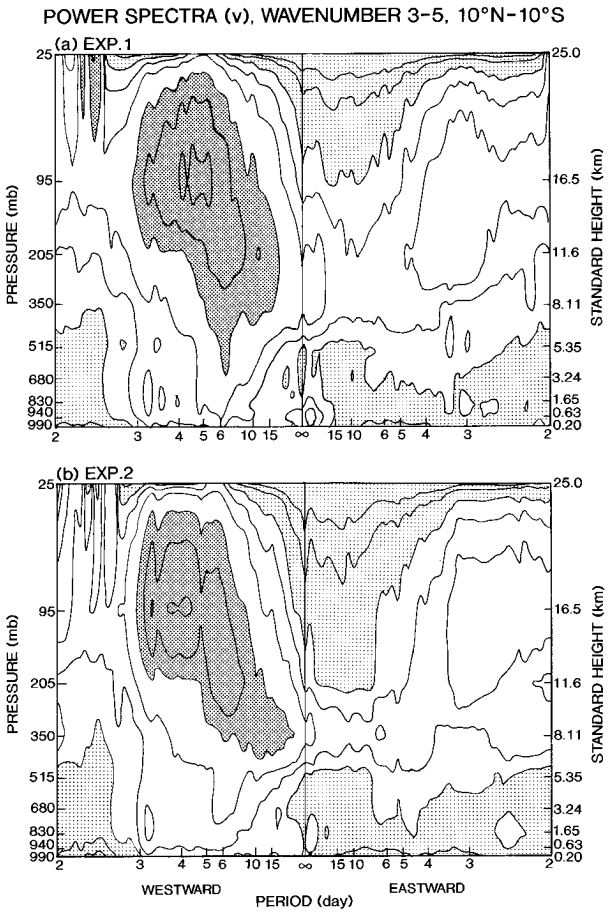

FIG. 5. Frequency–height distributions of the space–time wavenumbers 3–5 power spectral density of the equatorially symmetric meridional velocity averaged between 10°N and 10°S for (a) experiment 1 and (b) experiment 2. Contour values: 0.1. 0.2, 0.5, 1, 2, 5, 10, and 20 $(\text{m s}^{-1})^2$ day. Dark shading indicates values greater than 5.0, light shading less than 0.5.

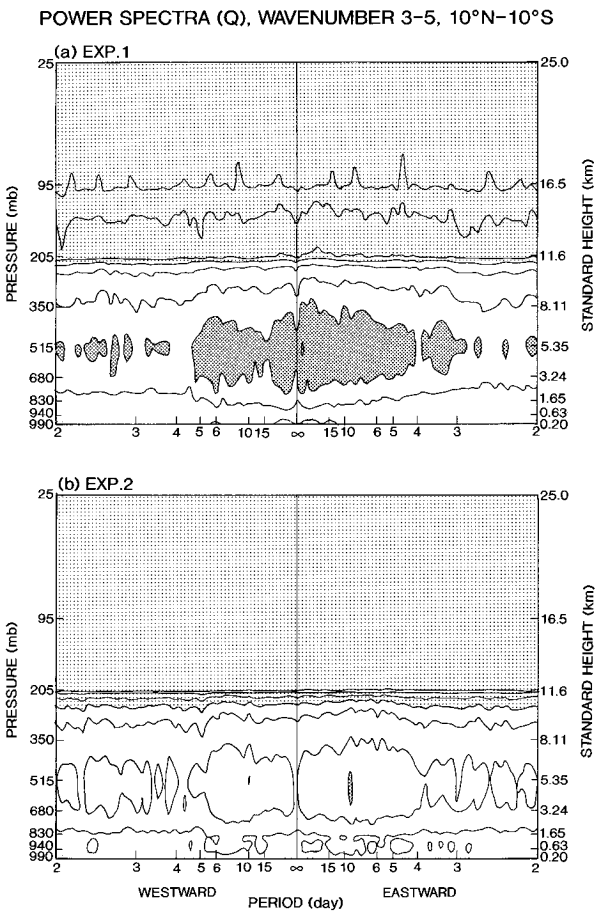

FIG. 6. As in Fig.5 except for the equatorially antisymmetric MCA heating (Q). Contour values: 0.01, 0.02, 0.05, 0.1, 0.2, 0.5, 1, and 2 $(\text{K day}^{-1})^2$ day. Dark shading indicates values greater than 1.0, light shading less than 0.1.

eastward-moving periods of 40–50 days, corresponding to the 40–50-day TIO. Comparison between Figs. 4a (experiment 1) and 4b (experiment 2) indicates that the TIO peak is profoundly weakened by the wind-feedback removal. On the other hand, a distinct 10–15-day peak, which would correspond to the stratospheric Kelvin wave, is not seen in the MCA heating spectra.

f. Mixed Rossby–gravity waves

Figures 5a and 5b are based on experiments 1 and 2, respectively, displaying the frequency–height distributions of the space–time wavenumber 3–5 power spectral density of the equatorially symmetric meridional velocity, which has been averaged between 10°N and 10°S. The stratospheric spectral peak found at westward moving periods of 4–6 days corresponds to MRG waves (Yanai and Maruyama 1966). Comparison between Figs. 5a and 5b indicates that the MRG wave is not appreciably reduced by wind-feedback removal. This result demonstrates that the MRG wave in experiment 1, like the Kelvin wave, is maintained almost entirely through the ST mechanism. In both Figs. 5a and 5b, the dominant period of the wavenumber 3–5 MRG waves in the upper troposphere is 5–10 days, shifting to 3–5 days in the lower stratosphere. The shift of MRG wave frequencies with height can also be found in a realistic GFDL SKYHI model and the First GARP (Global Atmospheric Research Project) Global Experiment data (Hayashi and Golder 1994). The multiple frequencies suggest that not only Kelvin waves but also MRG waves consist of multiple vertical modes.

Fiqures 6a and 6b are the same as Figs. 5a and 5b, respectively, except for the antisymmetric MCA heating (Q). A distinct 3–5-day peak, which would correspond to stratospheric MRG waves, does not appear in the MCA heating spectra. The heating spectra are uniformly reduced over all frequencies by the wind-feedback removal.

g. Superclusters

Observed superclusters (Nakazawa 1988; Hayashi and Nakazawa 1989) have a half-wavelength of 2000–

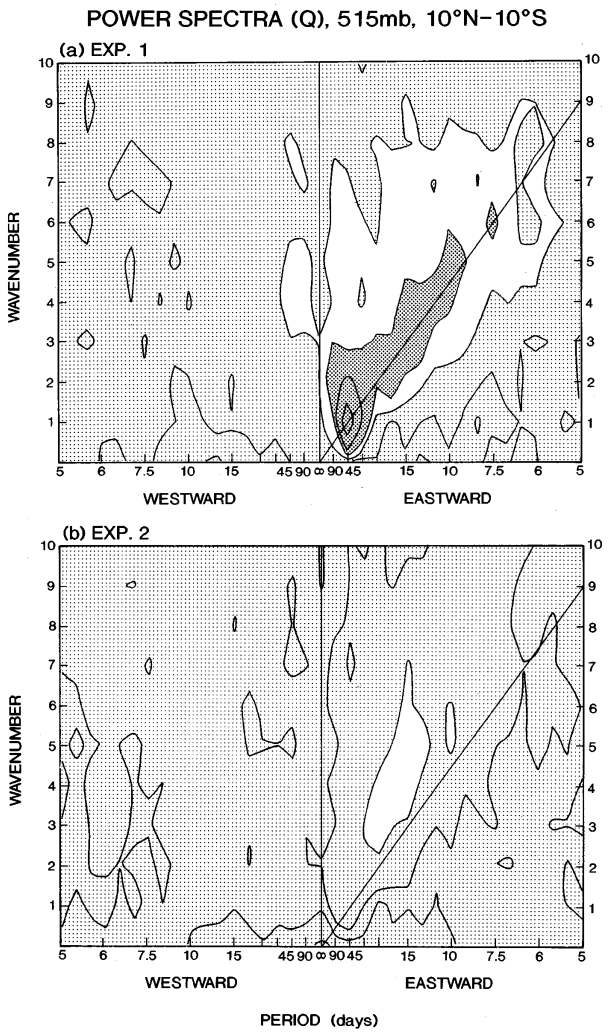

FIG. 7. Wavenumber–frequency distributions of the space–time power spectral density of the equatorially symmetric 515-mb MCA heating, which is averaged between 10°N and 10°S. Contour values: 0.02, 0.05, 0.1, 0.2, 0.5, 1, 2, and 5 $(K\ day^{-1})^2$ day. Dark shading indicates values greater than 1, light shading less than 0.

4000 km (wavenumbers 5–10) and periods of 5–15 days, propagating eastward with phase speeds of 5–10 m s^{-1} in the western Pacific. On the other hand, observed TIOs have local phase speeds of 5–10 m s^{-1} in the western Pacific and 10–15 m s^{-1} in less convectively active regions. The TIOs consist of several superclusters, which in turn consist of westward-moving cloud clusters having a half-wavelength of 100–500 km (Nakazawa 1988; Mapes and House 1993). Recently, Takayabu (1994a,b) and Takayabu et al. (1996) have observationally interpreted the westward moving quasi-2-day cloud clusters as westward-moving gravity waves.

Figures 7a and 7b are based on experiments 1 and 2, respectively, showing the wavenumber–frequency spectral distribution of the space–time power spectra of the symmetric 515-mb MCA heating (Q). The slanted line in each figure indicates an eastward phase velocity of 10 m s^{-1}, corresponding to that of the 40–50-day TIO. The power spectra distributed over the broad eastward-moving range of wavenumbers 3–10 and periods of 10–30 days correspond to superclusters. The simulated superclusters have a slightly slower phase speed than the simulated 40–50-day TIO. Comparison between these figures indicates that the MCA heating associated with the 40–50-day TIO is profoundly reduced by the wind-feedback removal, whereas that associated with the superclusters is not substantially reduced.

To visualize the zonal propagation of superclusters, Figs. 8a and 8b display equatorial longitude–time distributions over a period of one year (the fifth year) of the daily averaged precipitational heating in experiments 1 and 2, respectively. Both figures reveal the eastward propagation (indicated by the 5 and 10 m s^{-1} arrows) of superclusters consisting of grid-scale precipitation that mimics cloud clusters. It is difficult to detect TIOs without space–time smoothing. Comparison between these figures indicates that superclusters are not appreciably reduced by the wind-feedback removal.

Since it is difficult in Figs. 8a and 8b to see any detailed time variation of grid-scale precipitation, Figs. 9a and 9b show the equatorial longitude-time distributions of the 515-mb convective heating Q over the last 90 days of the fifth year for experiments 1 and 2, respectively. In these figures, it is seen that episodic convective heating occurs randomly. The TIOs cannot visually be detected in these figures without space–time smoothing. In the high-horizontal-resolution (1°) GFDL SKYHI model with MCA, episodic convective heating appears to move both eastward and westward (Hayashi and Golder 1994). If the horizontal resolution is sufficiently increased, episodic heating might better resemble the westward-moving cloud clusters observed by Nakazawa (1988). Comparison between Figs. 9a (experiment 1) and 9b (experiment 2) indicates that grid-scale waves are not appreciably reduced by the wind-feedback removal.

Figures 10a and 10b are the same as Figs. 9a and 9b, respectively, except for the 515-mb vertical pressure velocity, where contours are drawn only for upward motion. Both experiments 1 and 2 exhibit superclusters consisting of grid-scale episodic upward vertical motion, corresponding to episodic MCA heating. In addition, the vertical velocity has grid-scale components consisting of a pair of upward (shown) and downward (not shown) velocities. It is speculated that these components are associated with gravity waves, which are triggered by the episodic MCA heating (Figs. 9a,b) and then propagate in both eastward and westward directions. Comparison between Figs. 10a (experiment 1) and 10b (experiment 2) indicates that these ''gravity wave'' components are not appreciably reduced by the wind-feedback removal.

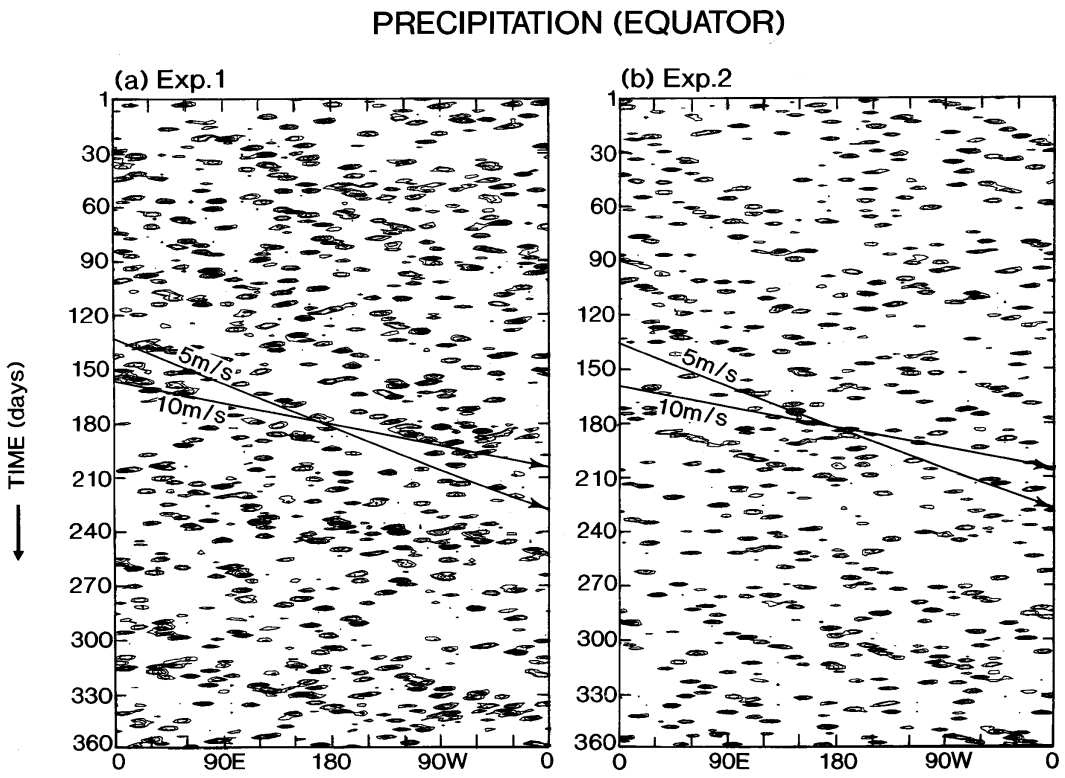

FIG. 8. Longitude–time diagrams over a period of 1 year of the daily averaged equatorial precipitational heating (year 5) for (a) experiment 1 and (b) experiment 2. The two arrows indicate eastward phrase velocities of 5 and 10 m s^{-1}. Contour values: 0.5, 1, 2, 3, 4, 5, 6, 7, and 8 (484 W m^{-2}).

h. Additional experiments

The present idealized model exhibits a pronounced wavenumber 1 40–50-day spectral peak but does not reveal a 25–30-day peak that appears strongly in realistic models and weakly in observed data (Hayashi and Golder 1993). There is the possibility that the dominance of the 40–50-day peak in the present model results from the unrealistically weak tropospheric static stability due to excessively low temperatures in the upper troposphere. To examine this possibility, the idealized model was modified by replacing the latitudinally uniform insolation and gaseous absorbers based on equatorial values with those based on values at 20°N. As will be shown in a subsequent paper, this modification resulted in the upper troposphere having fairly realistic temperatures and both 40–50 and 25–30 day peaks having comparable magnitudes. The result of wind-feedback removal from this modified model indicates that almost 90% of the kinetic energy of the 40–50-day TIO is maintained through the EWF mechanism, as was found in the present model. On the other hand, about 70% of the kinetic energy of the 25–30-day TIO is maintained through the EWF mechanism. The result for the 25–30-day TIO is consistent with that from the experiment by Neelin et al. (1987), based on an idealized R15 model having a zonally uniform distribution of sea surface temperatures. The ST mechanism for the 25–30-day TIO, however, could be exaggerated in low-resolution idealized models.

In order to clarify the relative roles of the latent and sensible heat fluxes, wind fluctuations in the surface fluxes of latent and sensible heat were separately eliminated from the idealized model. The wind-feedback removal in the latent heat flux was found to have a much greater effect on the kinetic energy of TIOs than that of the sensible heat flux.

The effect of convergence feedback on simulated transient waves in the presence of the EWF mechanism was also examined by removing this effect from experiment 1 instead of experiment 2. It was found that transient kinetic energy was substantially reduced in the absence of convergence feedback, which affects not only the ST mechanism but also the EWF mechanism.

To examine the effect of condensational heating, MCA was eliminated from the idealized model, leaving the dry-adjustment process unmodified. It was found that tropical transient waves were drastically weakened but did not completely disappear. Subsequently, when wind fluctuations in the surface flux of sensible heat were eliminated from the dry model, all waves completely disappeared. This result demonstrates that, even in the absence of moist convection, tropical transient

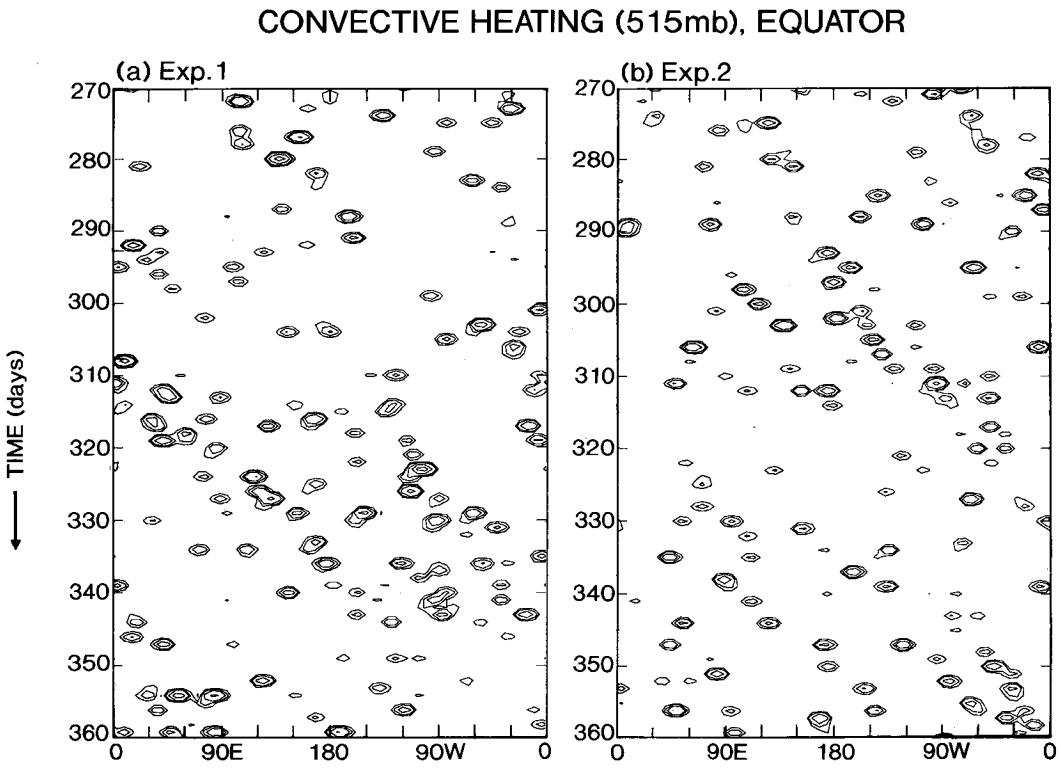

FIG. 9. Longitude–time diagrams over the last 90 days of the year-5 515-mb equatorial heating due to convective adjustment for (a) experiment 1 and (b) experiment 2. Contour values: 5, 10, 20, 50, and 100 (K day^{-1}).

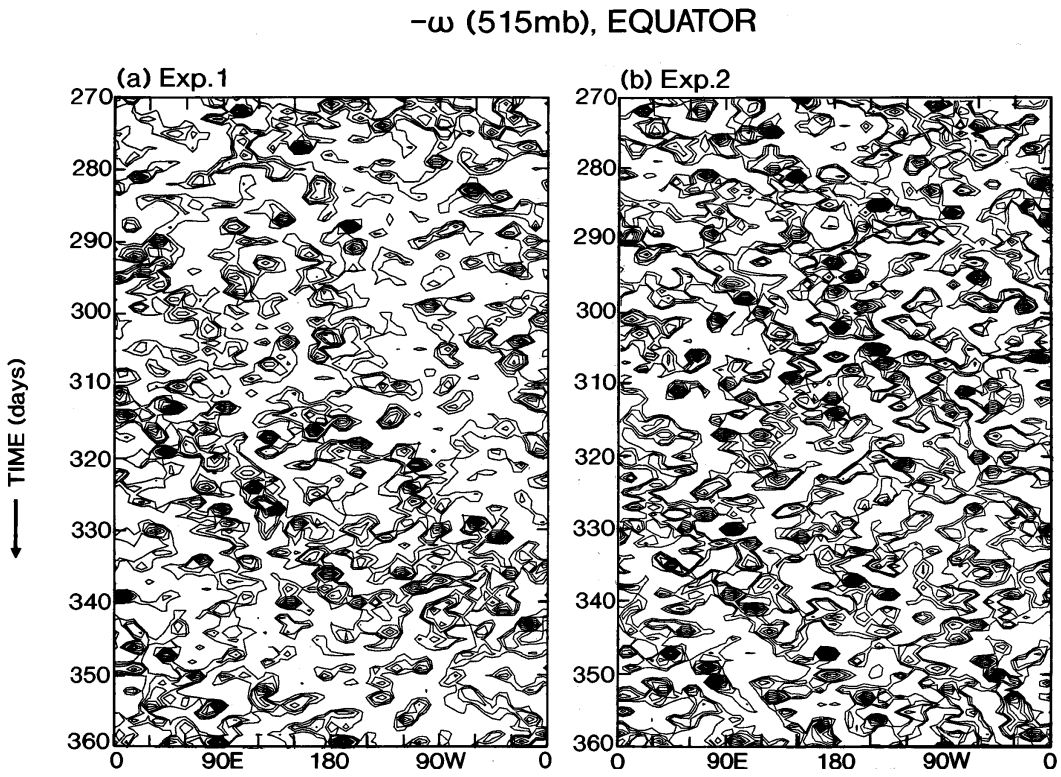

FIG. 10. As in Fig. 9 except for the 515-mb equatorial vertical pressure velocity (sign reversed). Contours are drawn only for upward motion. Contour values: 0.05, 0.5, 1, 2, 3, 4, 5, 6, 7, 8, 9, and 10 (0.1 Pa s^{-1}).

waves can be qualitatively generated through the coupling between waves and dry convection, being destabilized through the feedback between winds and the sensible heat flux.

4. Discussion

The present results are based on the MCA scheme that turns off moist convection during periods when large-scale moisture becomes unsaturated. This turn-off condition may be too strict, since moist convection can occur in the real atmosphere even when the environment is unsaturated. Nevertheless, this condition assures that condensation occurs at the lifting condensation level (LCL; see Holton 1992, 288). In order for moist convection to occur, subcloud air parcels must be somehow lifted above the LCL to become saturated and further lifted above the level of free convection (LFC) to become buoyant. When the lifting is primarily due to short-period gravitv waves, the vertical motion changes direction over the wave period, resulting in an upper limit that a subcloud-layer parcel can reach before it descends. There could be random lifting mechanisms in the atmosphere, but they do not necessarily trigger moist convection unless the low-level parcel reaches the LFC.

Other schemes, such as those proposed by Gadd and Keers (1970), Kurihara (1973), Arakawa and Schubert (1974), and Emanuel (1991), do not assume a critical value of relative humidity below which parameterized moist convection is suppressed, regardless of the stratification. It follows that the other schemes do not allow the stratification to become unstable during periods of subcritical relative humidity and therefore do not allow the ST mechanism. If an inversion layer exists at low levels, however, the Arakawa–Schubert (AS) scheme allows a conditionally unstable stratification above the inversion layer, since the AS scheme is not applied above this layer. If the MCA scheme is additionally applied to neutralize any conditionally unstable stratification above this layer, the ST mechanism is allowed, even in a model having the AS scheme. Moreover, if critical relative humidity is incorporated, the ST mechanism is allowed, even in models employing the other schemes.

Except for the assumption of critical relative humidity, the ST mechanism can be interpreted in a less parameterization-dependent context, since the first and second MCA processes defined in section 2b are qualitatively present in the other schemes. For example, the first and second MCA processes are analogous to the initial (i.e., nonequilibrium) and quasi-equilibrium adjustment processes, respectively, in the AS scheme with prognostic adjustment (Arakawa and Xu 1992; Randall and Pan 1993).

The other schemes do not always adjust or relax the moisture and lapse rate to the respective saturated and conditionally neutral values. For example, the Gadd–Keers scheme empirically relates the critical lapse rate for the onset of MCA to relative humidity, while the Kurihara scheme objectively relates the critical lapse rate to relative humidity through the effect of entrainment. The AS scheme also has an implicit relationship between the critical lapse rate and relative humidity through lifting condensation and entrainment (see Arakawa and Chen 1987).

The present experiments have demonstrated that no mechanism other than the EWF, ST, and lateral triggering mechanisms exists in the present idealized model having the original MCA scheme. On the contrary, Hu and Randall (1994, 1995) demonstrated, using one-dimensional radiative–convective models having either the MCA scheme modidfied by Randall et al. (1989) or a simplified AS scheme, that nonlinear interactions among radiation, convection, and the surface moisture flux can result in a new mechanism for the 30–60 day TIO. This mechanism probably depends on the fact that their models allow the lapse rate and relative humidity to oscillate. In contrast to the original MCA scheme, the modified MCA scheme allows the lapse rate to deviate from the moist adiabat, even during periods of moist convection. The deviation is due to the fact that the large-scale condensation process is allowed after the modified scheme first adjusts the lapse rate to the moist adiabat, whereas the original MCA scheme simultaneously adjusts temperature and moisture. The modified scheme, however, does not allow the ST mechanism, in spite of the fact that the large-scale condensation process is turned on at the onset of saturation. This is due to the lapse rate being always adjusted to the moist adiabat, even during periods of nonsaturation.

5. Conclusions and remarks

To examine several mechanisms for the generation of low- and high-frequency tropical waves, numerical experiments were conducted with the use of an idealized nine-level R21 spectral general circulation model having the original scheme of moist convective adjustment (MCA). This model prescribes globally uniform, time-independent distributions of sea surface temperatures of 300 K and equinox insolation conditions, thereby excluding stationary waves and extratropical baroclinic waves. The results are summarized as follows:

1) Experiment 1 (control) produced intraseasonal oscillations, superclusters, Kelvin waves, and mixed Rossby–gravity waves in the idealized model.
2) Experiment 2 eliminated the evaporation–wind feedback (EWF) mechanism from the idealized model by suppressing wind fluctuations in the parameterized surface flux of latent and sensible heat. The intraseasonal oscillations were profoundly weakened, while other waves were not substantially weakened.
3) Experiment 3 eliminated the wave-CISK mechanism from experiment 2 by suppressing ''convergence feedback,'' which is part of moisture convergence.

All waves were substantially weakened, but did not completely disappear. This result demonstrates that another mechanism must exist in the idealized model to generate wave energy in the absence of the wave-CISK, EWF, and lateral-triggering mechanisms.

4) Experiment 4 eliminated the EWF mechanism, as in experiment 2. This experiment also eliminated the saturation-triggering (ST) mechanism by modifying the original MCA scheme in such a way that MCA is allowed to occur even during periods of nonsaturation. The modified MCA scheme neutralizes any conditionally unstable stratification that would otherwise develop during periods of nonsaturation, thereby eliminating the ST mechanism. All waves disappeared in spite of the presence of convergence feedback. This result demonstrates that the transient waves in experiment 2 are generated through the ST mechanism. It also demonstrates that the MCA scheme does not allow wave-CISK that would generate wave energy in the absence of the EWF, ST, and lateral-triggering mechanisms.
5) Experiment 5 is the same as experiment 4, except that the ST mechanism was eliminated by modifying the process of dry convective adjustment, which is part of the MCA scheme, in such a way that the dry adiabat was replaced with the moist adiabat. As in experiment 4, the modified dry-adjustment process neutralizes any conditionally unstable stratification that would otherwise develop during periods of nonsaturation, thereby eliminating the ST mechanism. In contrast to experiment 4, however, experiment 5 retains the positive-only property of condensational heating. As in experiment 4, all waves disappeared, in spite of the presence of convergence feedback. This result demonstrates that preexisting unstable stratification is essential to the ST mechanism.

The above results are consistent with the united mechanisms proposed as follows, although the lateral-triggering mechanism was not presently examined. Intraseasonal oscillations are maintained primarily through the EWF mechanism, while other waves are maintained primarily through the ST mechanism and/or the lateral-triggering mechanisms. All these waves, however, can be qualitatively generated through either of these mechanisms.

The relative effects of the EWF and ST mechanisms could substantially depend on the idealized model and resolution as well as on convective schemes. Since the present results are based on the MCA hypothesis, they do not necessarily deny the existence of the wave-CISK mechanism in the real atmosphere. If both the wave-CISK and ST mechanisms exist in the real atmosphere, all existing convective schemes must be improved to adequately simulate tropical transient waves.

In a subsequent paper (Hayashi and Golder 1997), the united mechanisms will be theoretically interpreted. Further experiments will be conducted to clarify the effects of realistic static stability and the nonlinear effects of evaporation and condensation on the united mechanisms. In the future, these mechanisms will be reexamined by use of a realistic high-resolution model.

Acknowledgments. The authors are grateful to Drs. S. Manabe and J. D. Mahlman for their advice and encouragement. Appropriate comments on the original manuscript were offered by Drs. I. M. Held, K. Hamilton, H. Itoh, and A. Numaguti. Valuable suggestions from anonymous reviewers are greatly appreciated.

APPENDIX

Definition of Convergence Feedback

The moisture-convergence terms can be written in advection form as

$$-\frac{\partial uq}{\partial x} - \frac{\partial vq}{\partial y} - \frac{\partial \omega p}{\partial p} = -u\frac{\partial q}{\partial x} - v\frac{\partial q}{\partial y} - \omega\frac{\partial q}{\partial p}, \quad \text{(A1)}$$

where q is the specific humidity, while u, v, and $\boldsymbol{\omega}$ are, respectively, the zonal, meridional, and vertical velocities in pressure coordinates. In deriving (A1), the continuity equation has been employed.

In the CISK parameterization (Ooyama 1964; Charney and Eliassen 1964), the horizontal moisture-advection terms in (A1) are neglected, and the moisture convergence terms are therefore approximated by the vertical moisture advection term.

When this term is vertically averaged, it can be rewritten as

$$-\left\langle \omega\frac{\partial q}{\partial p}\right\rangle = \left\langle \frac{\partial \omega}{\partial p}q\right\rangle, \quad \text{(A2)}$$

$$= -\left\langle \left(\frac{\partial u}{\partial x} + \frac{\partial v}{\partial y}\right)q\right\rangle, \quad \text{(A3)}$$

$$= -\frac{\omega(p_b)}{\Delta p}q(p_b), \quad \text{(A4)}$$

where angle brackets denote the vertical pressure average, p_b the pressure at the top of the subcloud layer, and Δp the pressure depth of the subcloud layer.

In deriving (A2) through integration by parts, $\boldsymbol{\omega}$ is assumed to vanish at the lower and upper boundaries. In deriving (A3) from (A2), the continuity equation has been used. In deriving (A4) from (A2), q is assumed to be concentrated in the subcloud layer and is approximated by a step function.

In the present paper, ''convergence feedback'' is defined as the zonal deviation of (A3), which is interpreted as the feedback of horizontal wind convergence to the vertically averaged moisture-convergence fluctuation.

REFERENCES

Arakawa, A., and W. H. Schubert, 1974: Interaction of a cumulus cloud ensemble with the large-scale environment. *J. Atmos. Sci.*, **31,** 674–701.

——, and J.-M. Chen, 1987. Closure assumptions in the cumulus parameterization problem. Short- and medium-range numerical weather prediction: Collection of papers presented at the WMO/IUGG NWP symposium, Tokyo, August 1986. *J. Meteor. Soc. Japan,* **65,** 107–131.

——, and K.-M. Xu, 1992: The macroscopic behavior of simulated cumulus convection and semi-prognostic tests of the Arakawa–Schubert cumulus parameterization. *Physical Process in Atmospheric Models,* O. R. Sikka and S. S. Singh, Eds., Wiley Eastern, 3–18.

Bates, J. R., A. M. Lasheen, and A. F. Hanna, 1978: On the application of the Arakawa–Schubert convective parameterization scheme. *J. Atmos. Sci.,* **35,** 1043–1046.

Bennet, J. R., and J. A. Young, 1971: The influence of latitudinal wind shear upon large-scale wave propagation into the tropics. *Mon. Wea. Rev.,* **99,** 202–214.

Betts, A. K., 1986: A new convective adjustment scheme. Part I: Observational and theoretical basis. *Quart. J. Roy. Meteor. Soc.,* **112,** 677–691.

——, and M. J. Miller, 1986: A new convective adjustment scheme. Part II: Single column tests using GATE waves, BOMEX, ATEX and arctic air-mass data sets. *Quart. J. Roy. Meteor. Soc.,* **112,** 693–709.

Blade, I., and D. L. Hartmann, 1993: Tropical intraseasonal oscillations in a simple nonlinear model. *J. Atmos. Sci.,* **50,** 2922–2939.

Boville, B. A., and W. J. Randel, 1992: Equatorial waves in a stratospheric GCM: Effects of vertical resolution. *J. Atmos. Sci.,* **49,** 785–801.

Bretherton, C. S., 1993: The nature of adjustment in cumulus cloud fields. *The Representation of Cumulus Convection in Numerical Models, Meteor. Monogr.,* No. 46, Amer. Meteor. Soc., 63–74.

——, and P. K. Smolarkiewicz, 1989: Gravity waves, compensating subsidence, and detrainment around cumulus clouds. *J. Atmos. Sci.,* **46,** 740–759.

Brown, R. G., and C. S. Bretherton, 1995: Tropical wave instabilities: Convective interaction with dynamics using the Emanuel convective parameterization. *J. Atmos. Sci.,* **52,** 67–82.

Chang, C. P., 1976: Forcing of stratospheric Kelvin waves by tropospheric heat sources. *J. Atmos. Sci.,* **33,** 740–744.

——, and H. Lim, 1988: Kelvin-wave CISK: A possible mechanism for the 30–50-day oscillations? *J. Atmos. Sci.,* **45,** 1709–1720.

Chao, W. C., 1995: A critique of wave-CISK as an explanation for the 40–50 day tropical intraseasonal oscillation. *J. Meteor. Soc. Japan,* **73,** 667–684.

——, and S.-J. Lin, 1994: Tropical intraseasonal oscillation, super cloud clusters, and cumulus convective schemes. *J. Atmos. Sci.,* **51,** 1282–1297.

——, and L. Deng, 1996: On the role of wind-induced surface heat exchange in a two-dimensional model of super cloud clusters. *J. Geophys. Res.,* **101,** 16 931–16 937.

Charney, J. G., 1969: A further note on large-scale motions in the tropics. *J. Atmos. Sci.,* **26,** 182–185.

——, and A. Eliassen, 1964: On the growth of hurricane depression. *J. Atmos. Sci.,* **21,** 68–75.

Cho, H.-R., 1994: Cloud clusters, Kelvin wave-CISK, and the Madden–Julian oscillations in the equatorial troposphere. *J. Atmos. Sci.,* **51,** 68–76.

Crum, F. X., and D. E. Stevens, 1983: A comparison of two cumulus parameterization schemes in a linear model of wave-CISK. *J. Atmos. Sci.,* **40,** 2671–2688.

——, and T. J. Dunkerton, 1992: Analytic and numerical models of wave-CISK with conditional heating. *J. Atmos. Sci.,* **49,** 1693–1708.

——, and ——, 1994: CISK and evaporation-wind feedback with conditional heating of an equatorial beta-plane. *J. Meteor. Soc. Japan,* **72,** 11–18.

Davey, M. K., 1989: A simple tropical moist model applied to the ''40-day'' wave. *Quart. J. Roy. Meteor. Soc.,* **115,** 1071–1107.

Davis, H. C., 1979: Phase-lagged wave-CISK. *Quart. J. Roy. Meteor. Soc.,* **105,** 323–353.

Dunkerton, T. J., and F. X. Crum, 1991: Scale selection and propagation of wave-CISK with conditional heating. *J. Meteor. Soc. Japan,* **69,** 449–458.

Emanuel, K. A., 1987: An air–sea interaction model of intraseasonal oscillations in the tropics. *J. Atmos. Sci.,* **44,** 2324–2340.

——, 1991: A scheme for representing cumulus convection in large-scale models. *J. Atmos. Sci.,* **48,** 2313–2335.

——, 1993: The effect of convective response time on WISHE modes. *J. Atmos. Sci.,* **50,** 1763–1775.

——, J. D. Neelin, and C. S. Bretherton, 1994: On large-scale circulations in convective atmosphere. *Quart. J. Roy. Meteor. Soc.,* **120,** 1111–1143.

Frederiksen, J. S., and C. S. Frederiksen, 1993: Monsoon disturbances, intraseasonal oscillations, teleconnection patterns, blocking, and storm tracks of the global atmosphere during January 1979: Linear theory. *J. Atmos. Sci.,* **50,** 1349–1372.

Gadd, A. J., and J. F. Keers, 1970: Surface exchanges of sensible and latent heat in a 10-level model atmosphere. *Quart. J. Roy. Meteor. Soc.,* **96,** 297–308.

Garcia, R. R., and M. L. Salby, 1987: Transient response to localized episodic heating in the tropics. Part II. Far-field behavior. *J. Atmos. Sci.,* **44,** 499–530.

Gordon, C. T., and W. F. Stern, 1982: A description of the GFDL global spectral model. *Mon. Wea. Rev.,* **110,** 625–644.

Goswami, P., and B. N. Goswami, 1991: Modification of $n = 0$ equatorial waves due to interaction between convection and dynamics. *J. Atmos. Sci.,* **48,** 2231–2244.

——, and ——, 1996: Reply. *J. Atmos. Sci.,* **53,** 919–922.

Hamilton, K., and J. D. Mahlman, 1988: General circulation model simulation of the semiannual oscillation of the tropical middle atmosphere. *J. Atmos. Sci.,* **45,** 3212–3235.

Hayashi, Y., 1970: A theory of large-scale equatorial waves generated by condensation heat and accelerating the zonal wind. *J. Meteor. Soc. Japan,* **48,** 140–160.

——, 1974: Spectral analysis of tropical disturbances appearing in a GFDL general circulation model. *J. Atmos. Sci.,* **31,** 180–218.

——, 1976: Non-singular resonance of equatorial waves under the radiation condition. *J. Atmos. Sci.,* **33,** 183–201.

——, 1982: Space-time spectral analysis and its applications to atmospheric waves. *J. Meteor. Soc. Japan,* **60,** 156–171.

——, and D. G. Golder, 1978: The generation of equatorial transient planetary waves: Control experiments with a GFDL general circulation model. *J. Atmos. Sci.,* **35,** 2068–2082.

——, and ——, 1980: The seasonal variation of tropical transient planetary waves appearing in a GFDL qeneral circulation model. *J. Atmos. Sci.,* **37,** 705–716.

——, and ——, 1986: Tropical intraseasonal oscillations appearing in a GFDL general circulation model and FGGE data. Part I: Phase propagation. *J. Atmos. Sci.,* **43,** 3058–3067.

——, and S. Miyahara, 1987: A three-dimensional linear response model of the tropical intraseasonal oscillation. *J. Meteor. Soc. Japan,* **65,** 843–857.

——, and D. G. Golder, 1988: Tropical intraseasonal oscillations appearing in a GFDL general circulation model and FGGE data. Part II: Structure. *J. Atmos. Sci.,* **45,** 3017–3033.

——, and ——, 1993: Tropical 40–50- and 25–30-day oscillations appearing in realistic and idealized GFDL climate models and the ECMWF dataset. *J. Atmos. Sci.,* **50,** 464–494.

——, and ——, 1994: Kelvin and mixed Rossby-gravity waves appearing in the GFDL ''SKYHI'' general circulation model and the FGGE dataset: Implications for their generation mechanism and role in the QBO. *J. Meteor. Soc. Japan,* **72,** 901–935.

——, and ——, 1997: United mechanisms for the generation of low- and high-frequency tropical waves. Part II: Theoretical interpretations. *J. Meteor. Soc. Japan,* in press.

——, ——, and J. D. Mahlman, 1984: Stratospheric and mesospheric Kelvin waves simulated by the GFDL ''SKYHI'' general circulation model. *J. Atmos. Sci.,* **41,** 1971–1984.

——, ——, ——, and S. Miyahara, 1989: The effect of horizontal resolution on gravity waves simulated by the GFDL SKYHI general circulation model. *Pure Appl. Geophys.,* **130,** 421–443.

Hayashi, Y.-Y., and A. Sumi, 1986: The 30–40 day oscillation simulated in an ''aqua-planet'' model. *J. Meteor. Soc. Japan,* **64,** 431–467.

——, and T. Nakazawa, 1989: Evidence of the existence and eastward motion of superclusters at the equator. *Mon. Wea. Rev.,* **117,** 236–243.

Held, I. M., R. S. Hemler, and V. Ramaswamy, 1993: Radiative–convective equilibrium with explicit two-dimensional moist convection. *J. Atmos. Sci.,* **50,** 3909–3927.

Hendon, H. H., 1988: A simple model of the 40–50-day oscillation. *J. Atmos. Sci.,* **45,** 569–584.

——, and B. Liebmann, 1991: The structure of annual variation of antisymmetric fluctuations of tropical convection and their association with Rossby–gravity waves. *J. Atmos. Sci.,* **48,** 2127–2140.

——, and M. L. Salby, 1996: Planetary-scale interactions forced by intraseasonal variations of observed convection. *J. Atmos. Sci.,* **53,** 1751–1758.

Hess, P., D. S. Battisti, and P. Rasch, 1993a: The maintenance of the intertropical convergence zones and the large-scale tropical circulation on a water covered earth. *J. Atmos. Sci.,* **50,** 691–713.

——, H. H. Hendon, and D. S. Battisti, 1993b: The relationship between mixed Rossby-gravity waves and convection in a general circulation model. *J. Meteor. Soc. Japan,* **71,** 321–338.

Holton, J. R., 1972: Waves in the equatorial stratosphere generated by tropospheric heat sources. *J. Atmos. Sci.,* **29,** 368–375.

——, 1973: On the frequency distribution of atmospheric Kelvin waves. *J. Atmos. Sci.,* **30,** 499–501.

——, 1992: *An Introduction to Dynamical Meteorology.* 3d. ed. Academic Press, 511 pp.

Horinouchi, T., and S. Yoden, 1996: Excitation of transient waves by localized episodic heating in the tropics and their propagation into the middle atmosphere. *J. Meteor. Soc. Japan,* **74,** 189–209.

Hu, Q., and D. A. Randall, 1994: Low-frequency oscillations in radiative-convective systems. *J. Atmos. Sci.,* **51,** 1089–1099.

——, and ——, 1995: Low-frequency oscillations in radiative–convective systems. Part II: An idealized model. *J. Atmos. Sci.,* **52,** 478–490.

Itoh, H., 1977: The response of equatorial waves to thermal forcing. *J. Meteor. Soc. Japan,* **55,** 222–239.

——, 1978: Forced equatorial waves under the marginally stable state with respect to the wave-CISK mechanism. *J. Meteor. Soc. Japan,* **56,** 145–158.

——, 1989: The mechanism for the scale selection of tropical intraseasonal oscillations. Part I: Selection of wavenumber 1 and the three-scale structure. *J. Atmos. Sci.,* **46,** 1779–1798.

——, 1994: Variations of atmospheric angular momentum associated with intraseasonal oscillations forced by zonally moving prescribed heating. *J. Geophys. Res.,* **99,** 12 981–12 998.

——, and M. Ghil, 1988: The generation mechanism of mixed Rossby-gravity waves in the equatorial troposphere. *J. Atmos. Sci.,* **45,** 585–604.

——, and N. Nishi, 1990: Consideration for the structure of the tropical intraseasonal oscillation. *J. Meteor. Soc. Japan,* **68,** 659–675.

Kuma, K., 1990: Diabatic heating and the low frequency dynamics in the tropics. *Meteor. Atmos. Phys.,* **44,** 265–279.

——, 1994: The Madden and Julian oscillation and the tropical disturbances in an aqua-planet version of the JMA global model with T63 and T156 resolution. *J. Meteor. Soc. Japan,* **72,** 147–172.

Kuo, H.-L., 1965: On formation and intensification of the tropical cyclones through latent heat release by cumulus convection. *J. Atmos. Sci.,* **22,** 40–63.

——, 1975: Instability theory of large-scale disturbances in the tropics. *J. Atmos. Sci.,* **32,** 2229–2245.

Kurihara, Y., 1973: A scheme of moist convective adjustment. *Mon. Wea. Rev.,* **101,** 547–553.

Lau, K.-M., and L. Peng, 1987: Origin of low frequency (intraseasonal) oscillations in the tropical atmosphere. Part I: Basic theory. *J. Atmos. Sci.,* **44,** 950–972.

——, and H.-T. Wu, 1994: Large scale dynamics associated with super cloud cluster organization over the tropical western Pacific. *J. Meteor. Soc. Japan,* **72,** 481–497.

——, ——, L. Peng, C.-H. Sui, and T. Nakazawa, 1989: Dynamics of super cloud clusters, westerly wind bursts, 30–60 day oscillations and ENSO: A unified view. *J. Meteor. Soc. Japan,* **67,** 205–219.

Lau, N.-C., and K.-M. Lau, 1986: The structure and propagation of intraseasonal oscillations appearing in a GFDL GCM. *J. Atmos. Sci.,* **43,** 2023–2047.

——, I. M. Held, and J. D. Neelin, 1988. The Madden–Julian oscillation in an idealized general circulation model. *J. Atmos. Sci.,* **45,** 3810–3932.

Lim, H., T.-K. Lim, and C.-P. Chang, 1990: Reexamination of wave-CISK theory: Existence and properties of nonlinear wave-CISK modes. *J. Atmos. Sci.,* **47,** 3078–3091.

Lindzen, R. S., 1967: Planetary waves on beta planes. *Mon. Wea. Rev.,* **95,** 441–451.

——, 1974: Wave-CISK in the tropics. *J. Atmos. Sci.,* **31,** 156–179.

——, and T. Matsuno, 1968: On the nature of a large-scale wave disturbances in the equatorial stratosphere. *J. Meteor. Soc. Japan,* **46,** 215–221.

Madden, R. A., and P. R. Julian, 1971: Detection of a 40–50 day oscillation in the zonal wind in the tropical Pacific. *J. Atmos. Sci.,* **28,** 702–708.

——, and ——, 1972: Description of global-scale circulation cells in the tropics with a 40–50 day period. *J. Atmos. Sci.,* **29,** 1109–1123.

——, and ——, 1994: Observations of the 40–50-day tropical oscillation—A review. *Mon. Wea. Rev.,* **122,** 814–837.

Mak, M. K., 1969: Laterally driven stochastic motions in the tropics. *J. Atmos. Sci.,* **26,** 41–64.

Manabe, S., J. Smagorinsky, and R. F. Stricler, 1965: Simulated climatology of a general circulation model with a hydrologic cycle. *Mon. Wea. Rev.,* **93,** 769–798.

——, D. G. Hahn, and J. L. Holloway Jr., 1979: Climate simulations with GFDL spectral models of the atmosphere: Effect of truncation. GARP Publ. Series 22, Vol. 1, 41–94. [Available from Secretariat of the World Meteorological Organization, No. 5, CH-1211 Geneva 20, Switzerland.]

Manzini, E., and K. Hamilton, 1993: Middle atmospheric traveling waves forced by latent heat and convective heating. *J. Atmos. Sci.,* **50,** 2180–2200.

Mapes, B. E., 1993: Gregarious tropical convection. *J. Atmos. Sci.,* **50,** 2026–2037.

——, and R. A. Houze Jr., 1993: Cloud clusters and superclusters over the oceanic warm pool. *Mon. Wea. Rev.,* **121,** 1398–1415.

Matsuno, T., 1966: Quasi-geostrophic motions in the equatorial area. *J. Meteor. Soc. Japan,* **44,** 25–43.

Miyahara, S., 1987: A simple model of the tropical intraseasonal oscillation. *J. Meteor. Soc. Japan,* **65,** 341–351.

——, Y. Hayashi, and J. D. Mahlman, 1986: Interaction between gravity waves and planetary-scale flow simulated by the GFDL SKYHI general circulation model. *J. Atmos. Sci.,* **43,** 1844–1861.

Nakajima, K., and T. Matsuno, 1988: Numerical experiments concerning the origin of cloud clusters in the tropical atmosphere. *J. Meteor. Soc. Japan,* **66,** 309–329.

Nakazawa, T., 1986: Intraseasonal variations of OLR in the tropics during the FGGE year. *J. Meteor. Soc. Japan,* **64,** 17–34.

——, 1988: Tropical super clusters within intraseasonal variations over the western Pacific. *J. Meteor. Soc. Japan,* **66,** 823–839.

Neelin, J. D., and J.-Y. Yu, 1994: Modes of tropical variability under convective adjustment and the Madden–Julian oscillation. Part I: Analytical theory. *J. Atmos. Sci.,* **51,** 1876–1894.

——, I. M. Held, and K. H. Cook, 1987: Evaporation-wind feedback and low-frequency variability in the tropical atmosphere. *J. Atmos. Sci.,* **44,** 2341–2348.

Nicholls, M. E., R. A. Pielke, and W. R. Cotton, 1991: Thermally forced gravity waves in an atmosphere at rest. *J. Atmos. Sci.,* **48,** 1869–1884.

Numaguti, A., and Y.-Y. Hayashi, 1991a: Behavior of cumulus activity and the structures of circulations in an ''aqua planet'' model. Part I: The structure of the super clusters. *J. Meteor. Soc. Japan,* **69,** 541–561.

——, and ——, 1991b: Behavior of cumulus activity and the structures of circulations in an ''aqua planet'' model. Part II: Eastward-moving

planetary scale structure and the intertropical convergence zone. *J. Meteor. Soc. Japan,* **69,** 563–579.
Ooyama, K., 1964: A dynamical model for the study of tropical cyclone development. *Geopfis. Int.,* **4,** 187–198.
Pandya, R., D. Durran, and C. Bretherton, 1993: Comments on ''Thermally forced gravity waves in an atmosphere at rest.'' *J. Atmos. Sci.,* **50,** 4097–4101.
Park, C.-K., D. M. Straus, and K.-M. Lau, 1990: An evaluation of the structure of tropical intraseasonal oscillations in three general circulation models. *J. Meteor. Soc. Japan,* **68,** 403–417.
Pitcher, E. J., and J. E. Geisler, 1987: The 40- to 50-day oscillation in a perpetual January simulation with a general circulation model. *J. Geophys. Res.,* **92,** 11 971–11 978.
Randall, D. A., and D.-M. Pan, 1993: Implementation of the Arakawa–Schubert cumulus parameterization with a prognostic closure. *The Representation of Cumulus Convection in Numerical Models, Meteor. Monogr.,* No. 46, Amer. Meteor. Soc., 137–144.
——, Harshvardhan, D. A. Dazlich, and T. G. Cosetti, 1989: Interactions among radiation, convection, and large-scale dynamics in a general circulation model. *J. Atmos. Sci.,* **46,** 1943–1970.
Randel, W., 1992: Upper tropospheric equatorial waves in ECMWF analyses. *Quart. J. Roy. Meteor. Soc.,* **118,** 365–394.
Riehl, H., 1954: *Tropical Meteorology.* McGraw Hill, New York, 392 pp.
Salby, M. L., and R. R. Garcia, 1987. Transient response to localized episodic heating in the tropics. Part I: Excitation and short-time near field behavior. *J. Atmos. Sci.,* **44,** 458–498.
——, ——, and H. H. Hendon, 1994: Planetary-scale circulations in the presence of climatological and wave-induced heating. *J. Atmos. Sci.,* **51,** 2344–2367.
Seager, R., and S. E. Zebiak, 1994: Convective interaction with dynamics in a linear primitive equation model. *J. Atmos. Sci.,* **51,** 1307–1331.
Sheng, J., 1996: The Madden–Julian oscillation in the Canadian Climate Centre general circulation model. *Climate Dyn.,* **12,** 125–140.
Slingo, J. M., and R. A. Madden, 1991: Characteristics of the tropical intraseasonal oscillation in the NCAR community climate model. *Quart. J. Roy. Meteor. Soc.,* **117,** 1129–1169.
——, and Coauthors, 1996: Intraseasonal oscillations in 15 atmospheric general circulation models: Results from an AMIP diagnostic subproject. *Climate Dyn.,* **12,** 325–357.
Stark, T. E., 1976: Wave-CISK and cumulus parameterization. *J. Atmos. Sci.,* **33,** 2387–2391.
Stevens, D. E., and R. S. Lindzen, 1978: Tropical wave-CISK with a moisture budget and cumulus friction. *J. Atmos. Sci.,* **35,** 940–961.
Sumi, A., 1992: Pattern formation of convective activity over the aqua-planet with globally uniform sea surface temperature (SST). *J. Meteor. Soc. Japan,* **70,** 855–876.
Swinbank, R. T., N. Palmer, and M. K. Davey, 1988: Numerical simulations of the Madden and Julian oscillations. *J. Atmos. Sci.,* **45,** 774–788.
Takahashi, M., 1987: A theory of the slow phase speed of the intraseasonal oscillation using wave-CISK. *J. Meteor. Soc. Japan,* **65,** 43–49.
——, 1993: A QBO-like oscillation in a two-dimensional model derived from a GCM. *J. Meteor. Soc. Japan,* **71,** 641–654.
——, and M. Shiobara, 1995: A note on a QBO-like oscillation in the 1/5 sector CCSR/NIES GCM. *J. Meteor. Soc. Japan,* **73,** 131–137.
Takayabu, Y. N., 1994a: Large-scale cloud disturbances associated with equatorial waves. Part I: Spectral feature of the cloud disturbances. *J. Meteor. Soc. Japan,* **72,** 433–449.
——, 1994b: Larqe-scale cloud disturbances associated with equatorial waves. Part II: Westward-propagating inertio-gravity waves. *J. Meteor. Soc. Japan,* **72,** 451–465.
——, K.-M. Lau, and C.-H. Sui, 1996: Observation of a quasi-2-day wave during TOGA COARE. *Mon. Wea. Rev.,* **124,** 1892–1913.
Tokioka, T., K. Yamazaki, A. Kitoh, and T. Ose, 1988: The equatorial 30–60-day oscillation and the Arakawa–Schubert penetrative cumulus parameterization. *J. Meteor. Soc. Japan,* **66,** 883–901.
Tsay, C.-Y., 1974: Analysis of large-scale wave disturbances in the tropics simulated by an NCAR global circulation model. *J. Atmos. Sci.,* **31,** 330–339.
Wallace, J. M., 1971: Spectral studies of tropospheric wave disturbances in the tropical western Pacific. *Rev. Geophys. Space Phys.,* **9,** 557–612.
——, 1973: General circulation of the tropical lower stratosphere. *Rev. Geophys. Space Phys.,* **11,** 191–222.
——, and V. E. Kousky, 1968: Observational evidence of Kelvin waves in the tropical stratosphere. *J. Atmos. Sci.,* **25,** 280–292.
Wang, B., 1988: Dynamics of the tropical low-frequency waves. An analysis of the moist Kelvin waves. *J. Atmos. Sci.,* **45,** 2051–2065.
——, and T. Li, 1994: Convective interaction with boundary-layer dynamics in the development of a tropical intraseasonal system. *J. Atmos. Sci.,* **51,** 1386–1400.
Webster, P. J., and H.-R. Chang, 1988: Equatorial energy accumulation and emanation regions: Impacts of a zonally varying basic state. *J. Atmos. Sci.,* **45,** 803–829.
Wilson, J. D., and M. Mak, 1984: Tropical response to lateral forcing with a latitudinally and zonally varying nonuniform basic state. *J. Atmos. Sci.,* **41,** 1187–1201.
Xie, S.-P., 1994: On the preferred zonal scale of wave-CISK with conditional heating. *J. Meteor. Soc. Japan,* **72,** 19–30.
——, A. Kubokawa, and K. Hanawa, 1993a: Evaporation-wind feedback and the organizing of tropical convection on the planetary scale. Part I. Quasi-linear instability. *J. Atmos. Sci.,* **50,** 3873–3883.
——, ——, and ——, 1993b: Evaporation-wind feedback and the organizing of tropical convection on the planetary scale. Part II. Nonlinear evolution. *J. Atmos. Sci.,* **50,** 3884–3893.
Xu, K.-M., 1993: Cumulus ensemble simulation. *The Representation of Cumulus Convection in Numerical Models, Meteor. Monogr.,* No. 46, Amer. Meteor. Soc., 221–235.
Yamagata, T., 1987. A simple moist model relevant to the origin of intraseasonal disturbances in the tropics. *J. Meteor. Soc. Japan,* **65,** 153–165.
——, and Y. Hayashi, 1984: A simple diagnostic model for the 30–50-day oscillation in the tropics. *J. Meteor. Soc. Japan,* **62,** 709–717.
Yamasaki, M., 1969: Large-scale disturbances in the conditionally unstable atmosphere in low latitudes. *Pap. Meteor. Geophys.,* **20,** 289–336.
——, 1977: A preliminary experiment of the tropical cyclone without parameterizing the effects of cumulus convection. *J. Meteor. Soc. Japan,* **55,** 11–31.
Yanai, M., 1975: Tropical meteorology. *Rev. Geophys. Space Phys.,* **13,** 685–710, and 800–808.
——, and T. Maruyama, 1966: Stratospheric wave disturbances propagating over the equatorial Pacific. *J. Meteor. Soc. Japan,* **44,** 291–294.
——, and M. Murakami, 1970: Spectrum analysis of symmetric and antisymmetric equatorial waves. *J. Meteor. Soc. Japan,* **48,** 186–197.
Yano, J. I., and K. Emanuel, 1991: An improved model of the equatorial troposphere and its coupling with the stratosphere. *J. Atmos. Sci.,* **48,** 377–389.
——, J. C. McWilliams, and M. W. Moncrief, 1995: Hiearchical tropical cloud systems in an analog shallow-water model. *J. Atmos. Sci.,* **52,** 1723–1742.
Yip, K.-J., and G. R. North, 1993: Tropical waves in a GCM with zonal symmetry. *J. Climate,* **6,** 1691–1702.
Yoshizaki, M., 1991: Selective amplification of the eastward-propagating mode in a positive-only wave-CISK model on an equatorial beta plane. *J. Meteor. Soc. Japan,* **69,** 353–373.
Yu, J.-Y., and J. D. Neelin, 1994: Modes of tropical variability under convective adjustment and the Madden–Julian oscillation. Part II: Numerical results. *J. Atmos. Sci.,* **51,** 1895–1914.
Zhang, C., 1993: Laterally forced equatorial perturbations in a linear model. Part II: Mobile forcing. *J. Atmos. Sci.,* **50,** 807–821.
——, and P. J. Webster, 1989: Effects of zonal flows on equatorially trapped waves. *J. Atmos. Sci.,* **46,** 3632–3652.
——, and ——, 1992: Laterally forced equatorial perturbations in a linear model. Part I: Stationary transient forcing. *J. Atmos. Sci.,* **49,** 585–607.